J|A|C|S COMMUNICATIONS

Published on Web 07/27/2010

A Combined Experimental−Computational Investigation of Carbon Dioxide Capture in a Series of Isoreticular Zeolitic Imidazolate Frameworks

William Morris,[†] Belinda Leung,[†] Hiroyasu Furukawa,[†] Omar K. Yaghi,[†] Ning He,[‡] Hideki Hayashi,[†] Yao Houndonougbo,[§] Mark Asta,[||] Brian B. Laird,[‡] and Omar M. Yaghi*,[†]

Center for Reticular Chemistry, Department of Chemistry and Biochemistry, University of California−Los Angeles, 607 Charles E. Young Drive East, Los Angeles, California 90095, Department of Chemistry, University of Kansas, Lawrence, Kansas 66045, Department of Chemistry and Biochemistry, Eastern Washington University, 226 Science Building, Cheney, Washington 99004, and Department of Materials Science and Engineering, University of California−Berkeley, 210 Hearst Memorial Mining Building, Berkeley, California 94720

Received May 11, 2010; E-mail: yaghi@chem.ucla.edu

Abstract: A series of five zeolitic imidazolate frameworks (ZIFs) have been synthesized using zinc(II) acetate and five different 4,5-functionalized imidazole units, namely ZIF-25, -71, -93, -96, and -97. These 3-D porous frameworks have the same underlying topology (RHO) with Brunauer−Emmet−Teller surface areas ranging from 564 to 1110 m^2/g. The only variation in structure arises from the functional groups that are directed into the pores of these materials, which include $-CH_3$, $-OH$, $-Cl$, $-CN$, $-CHO$, and $-NH_2$; therefore these 3-D frameworks are ideal for the study of the effect of functionality on CO_2 uptake. Experimental results show CO_2 uptake at approximately 800 Torr and 298 K ranging from 0.65 mmol g^{-1} in ZIF-71 to 2.18 mmol g^{-1} in ZIF-96. Molecular modeling calculations reproduce the pronounced dependence of the equilibrium adsorption on functionalization and suggest that polarizability and symmetry of the functionalization on the imidazolate are key factors leading to high CO_2 uptake.

Zeolitic imidazolate frameworks (ZIFs) are porous materials with structures based on 4-connected nets of zeolites wherein the metal ion and imidazolate replace the tetrahedral Si nodes and the oxide bridges, respectively.[1] ZIFs have been examined for their carbon dioxide capture and gas separation properties.[2] However, little is known about the factors influencing the uptake capacity of a ZIF material. One of the advantages of ZIF chemistry is the ability to employ variously functionalized links in the synthesis of their structures, without the interference of the functional groups in the synthesis of a target structure. Therefore, it is possible to make many ZIF structures, where each incorporates a different functionality but all have the same topology (isoreticular). This simplifies the task of relating gas uptake properties to the nature of the functional group in ZIF structures. Here, we report the synthesis, structure and carbon dioxide uptake properties of a series of ZIFs with crystal structures based on the zeolite RHO topology, with links that differ in their functionality. Specifically, the same synthetic procedure was used to produce ZIF-25, 71, 93, 96, and 97; built from the functionalized imidazoles, $C_5H_8N_2$ **dmeIm**, $C_3H_2N_2Cl_2$ **dcIm**, $C_5H_6N_2O$ **almeIm**, $C_4H_4N_4$ **cyamIm**, and $C_5H_8N_2O$ **hymeIm**, respectively (Scheme 1). We also report the results of computational studies on the carbon dioxide uptake behavior of this series, where the symmetry of the link and the polarizability of the functional group appear to have significant influence over the uptake capacity of a given ZIF structure.

In previous work, we[1,3] and others[4] have noted that imidazoles functionalized in the four and five positions tend to produce ZIFs that have a RHO topology that is constructed from a body-centered arrangement in which the largest cage has 48 vertices and 26 faces comprised of 6 octagons, 8 hexagons, and 12 squares (Scheme 1a). Therefore, in order to synthesize an isoreticular series of ZIFs, we selected the following 4,5 substituted imidazolate links: **dmeIm**, **dcIm**, **almeIm**, **cyamIm**, and **hymeIm** (Scheme 1b). The synthesis of each ZIF was achieved by mixing *N*,*N*-dimethylformamide (DMF) solutions of zinc acetate and the corresponding imidazole linker. For example, ZIF-93 was synthesized by dissolving **almeIm** (0.022 g, 0.20 mmol) in 10 mL of DMF and zinc acetate (0.145 g, 0.80 mmol) in 4 mL of DMF. The two solutions were mixed in a 20-mL scintillation vial and heated at 85 °C for 12 h to form a crystalline powder.[5]

Scheme 1[a]

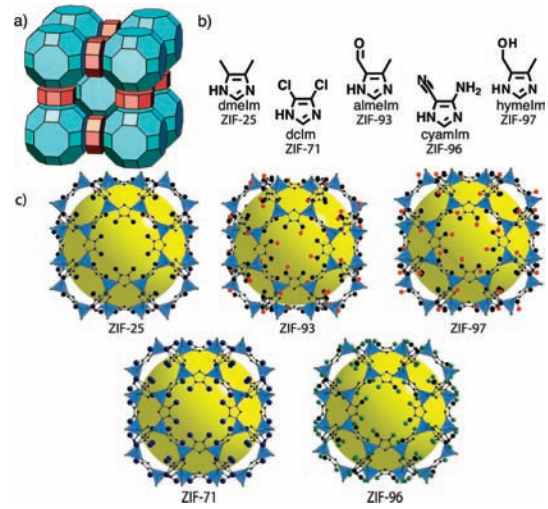

[a] (a) The tiling of the RHO structure representing the subdivisions of space (blue and red polyhedra). (b) The series of links **dmeIm**, **dcIm**, **almeIm**, **cyamIm**, and **hymeIm** used for the isoreticular ZIFs. (c) The structure of one cage that is linked together to make the structures of ZIF-25, -71, -93, -96, and -97. The yellow ball within the cage represents the free space. Atom colors: zinc, blue tetrahedra; carbon, black; chlorine, dark blue; oxygen, red; nitrogen, green. Hydrogen atoms are omitted for clarity. ZIF-25, -96, and -97 showed in ordered conformation.

Due to the isoreticular nature of these ZIF frameworks, it was possible to resolve their structures from the crystalline powders

[†] University of California−Los Angeles.
[‡] University of Kansas.
[§] Eastern Washington University.
[||] University of California−Berkeley.

10.1021/ja104035j

obtained (Figure 1). Powder X-ray diffraction (PXRD) data were collected for each ZIF; these patterns were compared to that calculated for ZIF-71 using single crystal X-ray data and found to have the same RHO topology. A Rietveld refinement of the experimental data of each structure was also performed to confirm that all the members of the ZIF series are based on the RHO topology.[5] These structures vary only in the organic functional groups which are found to be directed into the pore (Scheme 1c).

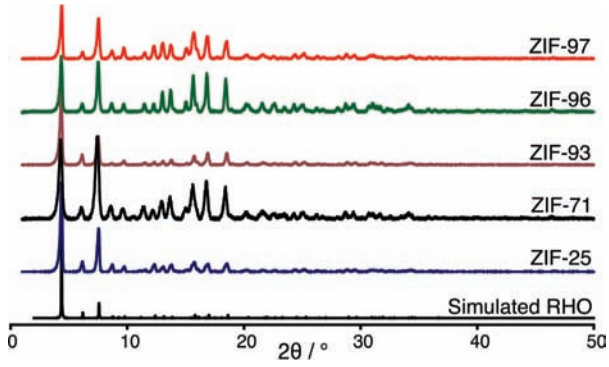

Figure 1. (a) PXRD patterns of activated ZIF-25 (blue), -71 (black), -93 (brown), -96 (green), and -97 (red). A simulated RHO pattern from single crystal data (black).[3]

To further characterize the ZIF materials, occluded solvent molecules were evacuated from the pores. ZIF-25, -71, and -93 were first washed with DMF (3 × 10 mL) over a 2 h period. Second, over a 3 day period the DMF was replaced with $CHCl_3$ (3 × 10 mL). The solvent-exchanged framework was then placed under a vacuum (30 mTorr) at 100 °C for 24 h. Similar procedures were followed for ZIF-96 and -97, but diethyl ether was used instead of $CHCl_3$. The compositions of these activated ZIFs are consistent with the elemental microanalyses performed.[6]

To verify that the functionalities have been successfully incorporated in each of the ZIF structures, solid state ^{13}C cross-polarization magic angle spinning (CP/MAS) NMR measurements were performed on the activated samples.[5] The spectra show the presence of the respective functionalities. We observe the $-CH_3$ functionality of ZIF-25, -93, and -97 at 9, 11, and 11 ppm, respectively; the −CHO functionality at 180 ppm for ZIF-93; the −CN functionality at 80 ppm for ZIF-96; and the $-CH_2OH$ functionality at 60 ppm for ZIF-97. This analysis confirms the homogeneous nature of the samples, as no additional peaks are observed. FT-IR spectroscopy also confirms these findings through characteristic stretches related to each functionality; −CN and −CHO stretches are present at 2176 and 1669 cm^{-1} for ZIF-96 and -97, respectively.[5]

The architectural stability and porosity of activated ZIFs was assessed by measuring the N_2 adsorption isotherms at 77 K.[5] The behavior for all ZIFs is Type I, indicative of permanent microporosity. The surface area of each framework was calculated using the Brunauer-Emmet-Teller (BET) method and found to be 564, 652, 864, 960, and 1110 $m^2\ g^{-1}$ for ZIF-97, -71, -93, -96, and -25, respectively.

The CO_2 uptake for each ZIF was measured at 298 K (Figure 2). ZIF-96 shows the highest CO_2 uptake at 800 Torr of 2.18 mmol g^{-1}, whereas ZIF-71 shows the lowest uptake, 0.65 mmol g^{-1}.

We executed a series of computer simulations designed to probe the origins of the measured variations in CO_2 uptake arising from the changes in the functional groups. The simulations were based on the grand canonical Monte Carlo method[7] using the Towhee code.[8] For CO_2, we used the EPM2 force field of Harris and Yung[9] which was optimized to give good agreement with the experimental vapor−liquid coexistence curve.[9,10] The universal force field (UFF),[11] combined with Lorentz−Berthelot mixing rules, was used to construct the van der Waals (vdW) interactions between the atoms in the ZIFs and the CO_2 molecules. The UFF has been used in this manner with some success in recent simulations of gas adsorption and separation in other ZIFs.[12] Because CO_2 possesses a significant quadrupole moment, it is expected that framework charge-quadrupole interactions (CQI) will give rise to an important contribution to the equilibrium adsorptions. To model these electrostatic interactions, the framework charges were derived using the REPEAT algorithm,[13] involving fits to the electrostatic potentials computed for each ZIF structure from periodic density functional theory calculations based on the projector-augmented wave method[14] and the Perdew−Becke−Ernzerhof generalized-gradient approximation,[15] as implemented in the VASP code.[16] The charges and further simulation details can be found in the Supporting Information.

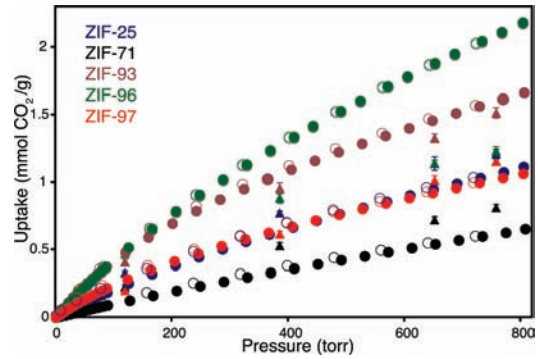

Figure 2. Experimental (circles) and simulated (triangles) CO_2 isotherms of each ZIF at 298 K: ZIF-25 (blue), -71 (black), -93 (brown), -96 (green), and -97 (red). Closed and open circles represent adsorption and desorption branches.

The simulation results for CO_2 adsorption isotherms at 298 K are plotted as a function of pressure (Figure 2) with the corresponding experimental results. With the notable exception of ZIF-96, the simulations predict the correct dependence of adsorptions on ZIF functionality and the magnitude of the adsorption within about 5 to 25% depending on the functionalization. The discrepancy between simulation and experiment in ZIF-96 is discussed further below. We have also calculated equilibrium CO_2 density maps for each of the five ZIF structures.[5] These maps indicate that, for pressures up to 750 torr, the primary absorption of CO_2 occurs at hexagonal faces of the large Linde Type A (*lta*) cavities (blue polyhedra in Scheme 1a). We also find secondary adsorption in the bridging double 8-fold rings (*d8r*) (red polyhedra in Scheme 1a); the adsorption at these sites is largest in magnitude for the frameworks that possess asymmetric functionalization on the imidazole rings, namely ZIF-93, -96, and -97. This adsorption is controlled primarily by electrostatic interactions, as the adsorption at these sites is reduced significantly in simulations where the framework charges are set to zero.

To examine the origins of the measured variations in CO_2 adsorption between the different ZIFs, we first consider the role of electrostatic interactions by calculating adsorptions with and without inclusion of the framework charges. The relative magnitude of the electrostatic interactions is found to correlate with the symmetry of the functionalization. For the frameworks with symmetric functionalization, ZIF-25 and -71, simulations with and without framework charges yield little difference in adsorption, whereas,

in the asymmetric ZIF-93, -96, and -97, inclusion of framework charges leads to an increase of up to two in the adsorption (Figure 3). This symmetry effect presumably reflects that, all other things being equal, the electrostatic field within a cavity generally decreases with increasing symmetry of the surface charge density. The differences between adsorption in symmetric and asymmetric ZIFs can be seen best by normalizing the adsorption by the pore surface area. The symmetric frameworks ZIF-25 and -71 have experimental CO_2 adsorptions at 750 Torr pressure of 0.90 and 0.98 μmol m^{-2}, whereas the same quantities for ZIF-93, -96, and -97 are considerably larger at 1.88, 2.21, and 1.84 μmol m^{-2}, respectively. To further test the correlation between symmetry and the effect of electrostatic interactions, we simulated a hypothetical asymmetric modification of ZIF-71, replacing one Cl on each imidazolate by an H atom (the position of which was optimized by DFT). At 298 K and a CO_2 partial pressure of 760 Torr, the electrostatic interactions in this asymmetric ZIF accounted for 19% of the total adsorption versus 9% for the symmetric ZIF-71, consistent with our hypothesis.

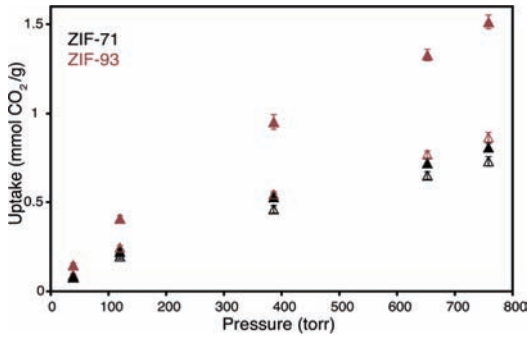

Figure 3. Effect of the electrostatic potential on the adsorption of CO_2 for ZIFs with symmetric (ZIF-71, black) and asymmetric (ZIF-93, brown) functionalization as calculated in the simulations. The open (filled) symbols represent calculations performed with the framework charges turned off (turned on). Other frameworks are shown in the Supporting Information for clarity.[5]

We considered next the role of the vdW interactions between framework and CO_2 atoms. As illustrated in Figure 3, simulations performed without the inclusion of framework charges, which probe only the short-range forces modeled by the UFF potentials, predict relatively small differences in CO_2 adsorption between the different ZIFs. The discrepancy between simulation and experiment in ZIF-96 points to a likely limitation of the UFF in describing the short-range vdW interactions. The UFF has a fixed single potential for each element, irrespective of bonding, to describe the vdW interaction between CO_2 and framework. For the nitrile and amine functional groups on the ZIF-96 imidazolate linker, the UFF considerably underestimates the strength of this vdW interaction compared with potentials that have been developed specifically for these functional groups.[17,18] As shown in the Supporting Information, when we replace the UFF vdW interactions for the nitrile and amine groups with those from the OPLS-ua potential,[18] we find that the simulated adsorption at 760 Torr and 298 K increases from 1.52 to 2.40 mmol g^{-1} (the experimental value is 2.11 mmol g^{-1}). This suggests that the adsorption is highly sensitive to the details of the vdW interactions and that more work is necessary to create a truly transferable potential for ZIFs. Also, the high adsorption of ZIF-96 relative to the other ZIFs studied is likely due to a combination of two effects: a large contribution arising from electrostatic interactions, due to the asymmetric functionalization, and strong vdW interactions arising from the polarizability of the functional groups.

In conclusion, we have synthesized a new series of isoreticular ZIFs with different pendant functionalities. Experimental studies supported by computational modeling show that the functionality's symmetry and polarizability significantly influence the CO_2 uptake capacity.

Acknowledgment. This material is based upon work supported as part of the Molecularly Engineered Energy Materials, an Energy Frontier Research Center funded by the U.S. Department of Energy, Office of Science, Office of Basic Energy Sciences under Award Number DE-SC0001342.

Supporting Information Available: Detailed experimental and modeling results. This material is available free of charge via the Internet at http://pubs.acs.org.

References

(1) Park, K. S.; Ni, Z.; Côté, A. P.; Choi, J. Y.; Huang, R.; Uribe-Romo, F. J.; Chae, H. K.; O'Keeffe, M.; Yaghi, O. M. *Proc. Natl. Acad. Sci. U.S.A.* **2006**, *103*, 10186–10191.
(2) Banerjee, R.; Furukawa, H.; Britt, D.; Knobler, C.; O'Keeffe, M.; Yaghi, O. M. *J. Am. Chem. Soc.* **2009**, *131*, 3875–3877.
(3) Banerjee, R.; Phan, A.; Wang, B.; Knobler, C.; Furukawa, H.; O'Keeffe, M.; Yaghi, O. M. *Science* **2008**, *319*, 939–943.
(4) (a) Liu, Y.; Kravtsov, V. Ch.; Larsen, R.; Eddaoudi, M. *Chem. Commun.* **2006**, 1488–1490. (b) Huang, X.-C.; Lin, Y.-Y.; Zhang, J.-P.; Chen, X. M. *Angew. Chem., Int. Ed.* **2006**, *45*, 1557–1559.
(5) See Supporting Information for full experimental data including synthetic conditions; powder X-ray diffraction; ^{13}C solid state NMR, FT-IR spectra; and additional simulation data.
(6) Elemental microanalysis percentages for activated samples; in parentheses calculated values: ZIF-25 Zn(**dmIm**)$_2$: C 46.45(46.98); H 5.60(5.52); N 21.74(21.92). ZIF-71 Zn(**dcIm**)$_2$: C 21.20(21.36); H 0.84(0.60); N 16.31(16.61), ZIF-93 Zn(**mealIm**)$_2$: C 42.01 (42.35); H 3.60(3.55); N 19.64(19.79). ZIF-96 Zn(**cyamIm**)$_2$: C 34.05(34.37); H 1.99(2.16); N 39.41(40.08). ZIF-97 Zn(**mehylIm**)$_2$·H_2O: C 40.01(39.29); H 5.11(5.28); N 18.68(18.33).
(7) Frenkel, D.; Smit, B. *Understanding Molecular Simulation*, 2nd ed.; Academic Press: New York, 2002.
(8) Martin, G. M.; Siepmann, J. I. *J. Phys. Chem. B* **1999**, *103*, 4508–4517.
(9) Harris, J.; Yung, K. *J. Phys. Chem.* **1995**, *99*, 12021–12024.
(10) Houndonougbo, Y. A.; Hong, J.; Rajagopalan, B.; Wong, K.; Kuczera, K.; Subramaniam, B.; Laird, B. *J. Phys. Chem. B* **2006**, *110*, 13195–13202.
(11) Rappe, A. K.; Casewit, C. J.; Colwell, K. S.; Goddard, W. A., III; Skiff, W. M. *J. Am. Chem. Soc.* **1992**, *114*, 10024–10035.
(12) (a) Rankin, R. B.; Liu, J.; Kulkarni, A. D.; Johnson, J. K. *J. Phys. Chem. C* **2009**, *113*, 16906–16914. (b) Liu, D.; Zheng, C.; Yang, Q.; Zhong, C. *J. Phys. Chem. C* **2009**, *113*, 5004–5009. (c) Perez-Pellitero, J.; Amrouche, H.; Siperstein, F. R.; Pirngruber, G.; Nieto-Draghi, C.; Chaplais, G.; Simon-Masseron, A.; Bazer-Bachi, D.; Peralta, D.; Bats, N. *Chem.—Eur. J.* **2010**, *16*, 1560–1571. (d) Sirjoosingh, A.; Alavi, S.; Woo, T. K. *J. Phys. Chem. C* **2010**, *114*, 2171–2178. (e) Liu, B.; Smit, B. *J. Phys. Chem. C* **2010**, *114*, 8515–8522.
(13) Campañá, C.; Mussard, B.; Woo, T. K. *J. Chem. Theory Comput.* **2009**, *5*, 2866–2878.
(14) Blöchl, P. *Phys. Rev. B* **1994**, *50*, 17953–17979.
(15) Perdew, J. P.; Burke, K.; Ernzerhof, M. *Phys. Rev. Lett.* **1996**, *77*, 3865–3868.
(16) (a) Kresse, G.; Furthmuller, J. *Phys. Rev. B* **1996**, *54*, 11169–11186. (b) Kresse, G.; Joubert, D. *Phys. Rev. B* **1999**, *59*, 1758–1775.
(17) Feng, X.-B.; Laird, B. B. *Mol. Phys.* **2005**, *103*, 2795–2801.
(18) Jorgensen, W. L.; Tirado-Rives, J. *J. Am. Chem. Soc.* **1988**, *110*, 1657–1666.

JA104035J